Lyapunov exponents for 2-D ray tracing without interfaces

Luděk Klimeš

Department of Geophysics, Charles University, Ke Karlovu 3, 121 16 Praha 2, Czech Republic, Fax: +420-2-2191 1214, E-mail: klimes@seis.karlov.mff.cuni.cz

Summary

The Lyapunov exponents asymptotically quantify the exponential divergence of rays. The "Lyapunov exponent" for a finite 2-D ray and the average "Lyapunov exponents" for a set of finite 2-D rays or lines and for a 2-D velocity model are introduced. The equations for the estimation of the average "Lyapunov exponents" in a given smooth 2-D velocity model without interfaces are proposed and illustrated by a numerical example. The equations allow to estimate the average exponential divergence of rays and exponential growth of the number of travel–time branches in the velocity model, prior to ray tracing.

Keywords

Velocity models, travel times, ray tracing, paraxial rays, deterministic chaos.

1 Introduction

If heterogeneities in a velocity model (macro model) exceed a certain degree, the average geometrical spreading exponentially increases with the length of rays and, in consequence, the average number of travel times exponentially increases with the distance from the source. Such a behaviour of rays strictly limits a possibility to calculate two–point rays and travel times in too complex models because:
(a) The geometrical spreading is as large as two–point rays cannot be found within the numerical accuracy. Similarly, the ray tubes cannot be sufficiently narrow for travel–time interpolation.
(b) The number of two–point travel times at each point is so large that the travel times cannot be calculated within reasonable computational time and costs.
(c) The number of two–point travel times at each point is so large that they can hardly be useful for any application, independently of the applicability of the ray theory which is not dealt with here.

It is thus of principal interest to quantify the exponential divergence of rays with respect to the complexity of the model, and to formulate explicit criteria enabling to construct models suitable for ray tracing.

The exponential divergence of rays is quantified by the Lyapunov exponents. Refer to the overview by Matyska (1999) for the introduction to the deterministic chaos and Lyapunov exponents with relevant references.

The aim of this paper is to estimate the "average Lyapunov exponent", describing the average spreading of ray tubes and average number of travel times, in smooth 2-D models without interfaces.

In: Seismic Waves in Complex 3-D Structures, Report 8 (Department of Geophysics, Charles University, Prague, 1999), pp. 83–96

2 Paraxial–ray propagator matrix

In this section, we consider 3-D space, but the form of the quantities and equations in 2-D (or N-D) space is obvious.

Let us denote by $\mathbf{w} = (x^1, x^2, x^3, p_1, p_2, p_3)^{\mathrm{T}}$ the phase-space coordinates. The ray tracing equations may be expressed in the form of

$$\frac{\mathrm{d}\mathbf{w}_\alpha}{\mathrm{d}\vartheta} = \Sigma_{\alpha\beta} \frac{\partial H}{\partial w^\beta} \quad , \tag{1}$$

where

$$\mathbf{\Sigma} = \begin{pmatrix} \mathbf{0} & \mathbf{1} \\ -\mathbf{1} & \mathbf{0} \end{pmatrix} \quad , \tag{2}$$

with $\mathbf{0}$ and $\mathbf{1}$ being the 3×3 (in 3-D space) zero and identity matrices, respectively. Here parameter ϑ along a ray is determined by the form of the Hamiltonian $H = H(w_\alpha)$.

The paraxial approximation of deviation $\delta\mathbf{w}(\vartheta)$ between the phase–space coordinates of the points of two infinitesimally close rays is

$$\delta\mathbf{w}(\vartheta) = \mathbf{\Pi}(\vartheta, \vartheta_0)\ \delta\mathbf{w}(\vartheta_0) \quad , \tag{3}$$

where $\delta\mathbf{w}(\vartheta_0)$ is the initial value of the deviation. Here $\mathbf{\Pi}$ is the *paraxial–ray propagator matrix*,

$$\Pi_{\alpha\beta}(\vartheta, \vartheta_0) = \frac{\partial w^\alpha(\vartheta)}{\partial w^\beta(\vartheta_0)} \quad . \tag{4}$$

The derivative of the paraxial–ray propagator matrix along a ray is given by the *dynamic ray tracing* equation

$$\frac{\mathrm{d}\mathbf{\Pi}(\vartheta, \vartheta_0)}{\mathrm{d}\vartheta} = \mathbf{\Sigma}\ \mathbf{H}(\vartheta)\, \mathbf{\Pi}(\vartheta, \vartheta_0) \quad , \tag{5}$$

where

$$H_{\alpha\beta} = \frac{\partial^2 H}{\partial w^\alpha \partial w^\beta} \tag{6}$$

are the second phase–space partial derivatives of the Hamiltonian. Dynamic ray tracing equation (5) directly follows from ray tracing equations (1) differentiated with respect to the initial conditions.

3 Lyapunov exponents

The Lyapunov exponents may be defined in several ways (Matyska 1999). Some definitions rely on unspecified norm $\|\bullet\|$ in phase space, which may be chosen arbitrarily. Although the phase–space norm does not influence the values of the Lyapunov exponents defined asymptotically for infinitely long rays, it may considerably influence the estimated values of the Lyapunov exponents along finite rays in finite models.

The estimations of the Lyapunov exponents based on the characteristic values of the paraxial–ray propagator matrix are not influenced by free parameters. On the other hand, the characteristic values are oscillating along rays which makes the estimation of the Lyapunov exponents difficult.

Let us denote μ_1, μ_2, ..., μ_{2N} the *characteristic values* of $2N \times 2N$ (in N-D space) propagator matrix $\mathbf{\Pi}$, i.e. the solutions of the characteristic equation

$$\det\left[\mathbf{\Pi}(\vartheta, \vartheta_0) - \mu(\vartheta, \vartheta_0)\mathbf{1}\right] = 0 \quad , \tag{7}$$

sorted according to their absolute values,

$$|\mu_1| \geq |\mu_2| \geq ... \geq |\mu_{2N}| \quad . \tag{8}$$

Complex–valued characteristic values, having the same absolute value, are assumed to be sorted according to their argument $-\pi < \arg\mu \leq \pi$. The characteristic values are also sometimes called eigenvalues. We prefer term characteristic values because the corresponding eigenvectors usually do not exist.

The *Lyapunov exponents* along a ray parametrized by monotonically increasing parameter σ may be defined as

$$\lambda_k = \limsup_{\vartheta\to+\infty} \frac{\ln|\mu_k(\vartheta,\vartheta_0)|}{\sigma(\vartheta)-\sigma(\vartheta_0)} \quad , \qquad k=1,2,...,N \quad , \tag{9}$$

see Matyska (1999). The Lyapunov exponents are thus defined with respect to a particular monotonic parameter $\sigma=\sigma(\vartheta)$ which may or may not differ from parameter ϑ determined by the form of the Hamiltonian.

Because of the symplectic property of the paraxial–ray propagator matrix, its inverse $\mathbf{\Pi}^{-1}$ has the same set of characteristic values as $\mathbf{\Pi}$. That is why the characteristic values of all Hamiltonian systems form reciprocal pairs $\mu_1\mu_{2N}=1$, $\mu_2\mu_{2N-1}=1$, ... $\mu_N\mu_{N+1}=1$. Each positive Lyapunov exponent of ray tracing (as of other Hamiltonian systems) is thus accompanied by the negative Lyapunov exponent of the same absolute value. It is thus sufficient to study the positive Lyapunov exponents for ray tracing.

4 Ray–centred coordinates

Assume that the Hamiltonian is a homogeneous function of the second order with respect to the slowness vector. Then the corresponding parameter along a ray is travel time, $\vartheta=\tau$. In the ray–centred coordinates, $\mathbf{w}^{(q)}=(q^1,q^2,q^3,p_1^{(q)},p_2^{(q)},p_3^{(q)})^{\mathrm{T}}$, the second phase–space derivatives of the Hamiltonian take the form of

$$\mathbf{H} = \begin{pmatrix} \multicolumn{2}{c}{\mathbf{H}_{11}} & \begin{smallmatrix}0\\0\end{smallmatrix} & \multicolumn{2}{c}{\mathbf{H}_{12}} & \begin{smallmatrix}0\\0\end{smallmatrix} \\ 0 & 0 & 0 & 0 & 0 & 0 \\ \multicolumn{2}{c}{\mathbf{H}_{21}} & \begin{smallmatrix}0\\0\end{smallmatrix} & \multicolumn{2}{c}{\mathbf{H}_{22}} & \begin{smallmatrix}0\\0\end{smallmatrix} \\ 0 & 0 & 0 & 0 & 0 & 1 \end{pmatrix} \quad , \tag{10}$$

and the paraxial–ray propagator matrix takes the form of

$$\mathbf{\Pi} = \begin{pmatrix} \multicolumn{2}{c}{\mathbf{Q}_{1}} & \begin{smallmatrix}0\\0\end{smallmatrix} & \multicolumn{2}{c}{\mathbf{Q}_{2}} & \begin{smallmatrix}0\\0\end{smallmatrix} \\ 0 & 0 & 1 & 0 & 0 & \tau \\ \multicolumn{2}{c}{\mathbf{P}_{1}} & \begin{smallmatrix}0\\0\end{smallmatrix} & \multicolumn{2}{c}{\mathbf{P}_{2}} & \begin{smallmatrix}0\\0\end{smallmatrix} \\ 0 & 0 & 0 & 0 & 0 & 1 \end{pmatrix} \quad , \tag{11}$$

see Klimeš (1994). Two characteristic values are thus units, $\mu_3=1$ and $\mu_4=1$, with the corresponding Lyapunov exponents identical to zero, $\lambda_3=0$ and $\lambda_4=0$.

Two positive Lyapunov exponents λ_1 and λ_2 correspond to 4×4 dynamic ray racing in the ray–centred coordinates, with matrices

$$\mathbf{H} = \begin{pmatrix} \mathbf{H}_{11} & \mathbf{H}_{12} \\ \mathbf{H}_{21} & \mathbf{H}_{22} \end{pmatrix} \quad , \qquad \mathbf{\Pi} = \begin{pmatrix} \mathbf{Q}_1 & \mathbf{Q}_2 \\ \mathbf{P}_1 & \mathbf{P}_2 \end{pmatrix} \quad . \tag{12}$$

Note that the ray–centred coordinates may be chosen in such a way that $\mathbf{H}_{12}=\mathbf{0}$ and $\mathbf{H}_{21}=\mathbf{0}$ in (12),

$$\mathbf{H} = \begin{pmatrix} \mathbf{H}_{11} & \mathbf{0} \\ \mathbf{0} & \mathbf{H}_{22} \end{pmatrix} \tag{13}$$

(Klimeš 1994). If we denote $\mathbf{H}_{11}=\mathbf{V}$ and $\mathbf{H}_{22}=\mathbf{G}$ in (13),

$$\mathbf{V}=\begin{pmatrix} \frac{\partial^2 H}{\partial q^1 \partial q^1} & \frac{\partial^2 H}{\partial q^1 \partial q^2} \\ \frac{\partial^2 H}{\partial q^1 \partial q^2} & \frac{\partial^2 H}{\partial q^2 \partial q^2} \end{pmatrix} \quad , \qquad \mathbf{G}=\begin{pmatrix} \frac{\partial^2 H}{\partial p_1^{(q)} \partial p_1^{(q)}} & \frac{\partial^2 H}{\partial p_1^{(q)} \partial p_2^{(q)}} \\ \frac{\partial^2 H}{\partial p_1^{(q)} \partial p_2^{(q)}} & \frac{\partial^2 H}{\partial p_2^{(q)} \partial p_2^{(q)}} \end{pmatrix} \quad , \tag{14}$$

the dynamic ray tracing equation takes the form of

$$\frac{\mathrm{d}}{\mathrm{d}\tau}\begin{pmatrix} \mathbf{Q}_1 & \mathbf{Q}_2 \\ \mathbf{P}_1 & \mathbf{P}_2 \end{pmatrix} = \begin{pmatrix} \mathbf{0} & \mathbf{G} \\ -\mathbf{V} & \mathbf{0} \end{pmatrix}\begin{pmatrix} \mathbf{Q}_1 & \mathbf{Q}_2 \\ \mathbf{P}_1 & \mathbf{P}_2 \end{pmatrix} \quad . \tag{15}$$

5 Positive Lyapunov exponent in 2-D

5.1 "Lyapunov exponent" of a finite ray

We decompose the 2×2 paraxial–ray propagator matrix $\mathbf{\Pi}$ into the 2×2 identity matrix $\mathbf{1}$ and the Pauli matrices

$$\boldsymbol{\sigma}_1=\begin{pmatrix} 0 & 1 \\ 1 & 0 \end{pmatrix} \ , \quad \boldsymbol{\sigma}_2=\begin{pmatrix} 0 & -\mathrm{i} \\ \mathrm{i} & 0 \end{pmatrix} \ , \quad \boldsymbol{\sigma}_3=\begin{pmatrix} 1 & 0 \\ 0 & -1 \end{pmatrix} \ , \tag{16}$$

which satisfy relations

$$\boldsymbol{\sigma}_1\boldsymbol{\sigma}_2=-\boldsymbol{\sigma}_2\boldsymbol{\sigma}_1=\mathrm{i}\boldsymbol{\sigma}_3 \ , \quad \boldsymbol{\sigma}_2\boldsymbol{\sigma}_3=-\boldsymbol{\sigma}_3\boldsymbol{\sigma}_2=\mathrm{i}\boldsymbol{\sigma}_1 \ , \quad \boldsymbol{\sigma}_3\boldsymbol{\sigma}_1=-\boldsymbol{\sigma}_1\boldsymbol{\sigma}_3=\mathrm{i}\boldsymbol{\sigma}_2 \tag{17}$$

and

$$\boldsymbol{\sigma}_1\boldsymbol{\sigma}_1=\boldsymbol{\sigma}_2\boldsymbol{\sigma}_2=\boldsymbol{\sigma}_3\boldsymbol{\sigma}_3=\mathbf{1} \ . \tag{18}$$

The decomposition of the real–valued matrix $\mathbf{\Pi}$ reads

$$\mathbf{\Pi}=\Pi_0\mathbf{1}+\Pi_1\boldsymbol{\sigma}_1+\Pi_2\mathrm{i}\boldsymbol{\sigma}_2+\Pi_3\boldsymbol{\sigma}_3 \quad , \tag{19}$$

where Π_0, Π_1, Π_2 and Π_3 are real–valued coefficients. Note that coefficients Π_1 and Π_2 are just formal. Reasonable physical meaning and units correspond to off–diagonal terms $\Pi_1+\Pi_2$ and $\Pi_1-\Pi_2$ of matrix $\mathbf{\Pi}$, not to isolated Π_1 nor Π_2. Since $\det\mathbf{\Pi}=1$, the coefficients satisfy equation

$$\Pi_0^2-(\Pi_1+\Pi_2)(\Pi_1-\Pi_2)-\Pi_3^2=1 \quad . \tag{20}$$

Since $\det\mathbf{\Pi}=1$, the greater characteristic value of matrix $\mathbf{\Pi}$ is

$$\mu_1=|\Pi_0|+\sqrt{\Pi_0^2-1} \quad . \tag{21}$$

Because the characteristic value is oscillating along the ray, we shall look for a different "norm" which could substitute the characteristic value. We require the "norm" to be independent of free parameters and of the length and time units. It is not acceptable to have different measure of ray divergence for the same ray expressed once in kilometres and other time in feet. Both the off–diagonal components of $\mathbf{\Pi}$ are dependent on the units (kilometres, feet), only their product is independent. However, since $\det\mathbf{\Pi}=1$, the product of the off–diagonal components contain no additional information to the diagonal components. The "norm" thus can depend only on the diagonal components of $\mathbf{\Pi}$, i.e., on coefficients Π_0 and Π_3. Characteristic value (21) is of little use at the points along a ray where Π_0 is small with respect to the other coefficients. We thus replace characteristic value (21) by "norm"

$$M=\sqrt{\Pi_0^2+\Pi_3^2}+\sqrt{\Pi_0^2+\Pi_3^2-1} \quad , \tag{22}$$

which is good also for small Π_0 and large Π_3. If both Π_0 and Π_3 are small, product $(\Pi_1 - \Pi_2)(\Pi_1 + \Pi_2)$ of the off–diagonal components is small, too, because of (20). "Norm" (22) can thus reasonably reflect the exponential ray divergence along the whole ray. We hope that "norm" (22) enables to define "Lyapunov exponents"

$$\lambda(\tau,\tau_0) = \frac{L(\tau,\tau_0)}{\sigma(\tau)-\sigma(\tau_0)} \tag{23}$$

for rays of finite lengths and to replace the limes superior in (9) by a simple limit,

$$\lambda = \lim_{\tau\to+\infty} \lambda(\tau,\tau_0) \quad . \tag{24}$$

Here we have denoted

$$L(\tau,\tau_0) = \ln\left[M(\tau,\tau_0)\right] \tag{25}$$

the function characterizing propagator matrix $\mathbf{\Pi}(\tau,\tau_0)$. Example of the dependence of $L(\tau,\tau_0)$ on τ for the rays shot from a point source is shown in Figure 5. The magnitude of the variation of the "Lyapunov exponents" from ray to ray is considerable and the "Lyapunov exponent" for a single ray obviously cannot be linked to the overall properties of the velocity model.

Fortunately, equation (23) allows to simply introduce average "Lyapunov exponent"

$$\overline{\lambda} = \frac{\sum\limits_{\mathrm{ray}} L_{\mathrm{ray}}(\tau,\tau_0)}{\sum\limits_{\mathrm{ray}}[\sigma_{\mathrm{ray}}(\tau)-\sigma_{\mathrm{ray}}(\tau_0)]} \tag{26}$$

over all rays. Such an average "Lyapunov exponent" express the global properties of the velocity model. However, for a single source, it is still dependent on the source geometry and position with respect the model boundaries. The average "Lyapunov exponent" over various sources should describe the global properties of the velocity model and should be dependent on the model boundaries just if the statistical properties of the model are anisotropic.

5.2 Approximation of the paraxial–ray propagator matrix

In 2-D, dynamic ray tracing equation (15) simplifies to equation

$$\frac{\mathrm{d}\mathbf{\Pi}}{\mathrm{d}\tau} = \begin{pmatrix} 0 & G \\ -V & 0 \end{pmatrix} \mathbf{\Pi} \quad . \tag{27}$$

The infinitesimal propagator matrix for small travel time increment $\delta\tau$ is

$$\mathbf{\Pi}_{\delta\tau} = \mathbf{1} + \begin{pmatrix} 0 & G \\ -V & 0 \end{pmatrix} \delta\tau + O(\delta\tau^2) \quad . \tag{28}$$

For $VG < 0$ ("high velocity") it reads

$$\mathbf{\Pi}_{\delta\tau} = \begin{pmatrix} |\frac{V}{G}|^{-\frac{1}{4}} & 0 \\ 0 & |\frac{V}{G}|^{\frac{1}{4}} \end{pmatrix} \left(\mathbf{1} + \boldsymbol{\sigma}_1\sqrt{-VG}\,\delta\tau\right) \begin{pmatrix} |\frac{V}{G}|^{\frac{1}{4}} & 0 \\ 0 & |\frac{V}{G}|^{-\frac{1}{4}} \end{pmatrix} + O(\delta\tau^2)\ , \tag{29}$$

for $VG > 0$ ("low velocity")

$$\mathbf{\Pi}_{\delta\tau} = \begin{pmatrix} |\frac{V}{G}|^{-\frac{1}{4}} & 0 \\ 0 & |\frac{V}{G}|^{\frac{1}{4}} \end{pmatrix} \left(\mathbf{1} + \mathrm{i}\boldsymbol{\sigma}_2\sqrt{VG}\,\delta\tau\right) \begin{pmatrix} |\frac{V}{G}|^{\frac{1}{4}} & 0 \\ 0 & |\frac{V}{G}|^{-\frac{1}{4}} \end{pmatrix} + O(\delta\tau^2)\ . \tag{30}$$

Note that

$$\begin{pmatrix} (|\frac{V}{G}+\delta(\frac{V}{G})|^{\frac{1}{4}} & 0 \\ 0 & |\frac{V}{G}+\delta(\frac{V}{G})|^{-\frac{1}{4}} \end{pmatrix} \begin{pmatrix} |\frac{V}{G}|^{-\frac{1}{4}} & 0 \\ 0 & |\frac{V}{G}|^{\frac{1}{4}} \end{pmatrix}$$

$$= \begin{pmatrix} [1+(\frac{V}{G})^{-1}\delta(\frac{V}{G})]^{\frac{1}{4}} & 0 \\ 0 & [1+(\frac{V}{G})^{-1}\delta(\frac{V}{G})]^{-\frac{1}{4}} \end{pmatrix} = \mathbf{1}+\boldsymbol{\sigma}_3\frac{1}{4}\frac{\delta(VG^{-1})}{VG^{-1}}+O(\delta\tau^2)\ . \quad (31)$$

We now introduce three parameters

$$\Lambda = \int \sqrt{\mathrm{neg}(VG)}\,\mathrm{d}\tau \quad , \quad (32)$$

$$\Phi = \int \sqrt{\mathrm{pos}(VG)}\,\mathrm{d}\tau \quad (33)$$

and

$$\Psi = \frac{1}{4}\ln(|VG^{-1}|) \quad . \quad (34)$$

Here

$$\mathrm{pos}(x) = \max(x,0) \quad , \qquad \mathrm{neg}(x) = -\min(x,0)$$

denote the positive and negative parts of x, respectively. Parameter Λ accounts for the exponential spreading of the ray tube in phase space and parameter Φ describes how the ray tube in phase space is twisted.

The product of infinitesimal propagator matrices (29) is then

$$\mathbf{\Pi}_{\Delta\Lambda} = ...(\mathbf{1}+\boldsymbol{\sigma}_1\delta\Lambda)(\mathbf{1}+\boldsymbol{\sigma}_3\delta\Psi)(\mathbf{1}+\boldsymbol{\sigma}_1\delta\Lambda)(\mathbf{1}+\boldsymbol{\sigma}_3\delta\Psi)...+O(\delta\tau^2) \quad (35)$$

and the product of infinitesimal propagator matrices (30) is

$$\mathbf{\Pi}_{\Delta\Phi} = ...(\mathbf{1}+\mathrm{i}\boldsymbol{\sigma}_2\delta\Phi)(\mathbf{1}+\boldsymbol{\sigma}_3\delta\Psi)(\mathbf{1}+\mathrm{i}\boldsymbol{\sigma}_2\delta\Phi)(\mathbf{1}+\boldsymbol{\sigma}_3\delta\Psi)...+O(\delta\tau^2) \quad . \quad (36)$$

Note that the values of $\delta\Lambda$, $\delta\Phi$ and $\delta\Psi$ in (35) and (36) are varying along the considered segment of a ray. If the segment of a ray extends across the whole "high–velocity" or "low–velocity" region, i.e., if $V=0$ at the endpoints of the segment, we assume that the distribution of parameter Ψ along the segment is roughly symmetric and that it does not considerably influence matrix products (35) and (36). Neglecting the multiplicands with Ψ, (35) and (36) simplify to

$$\mathbf{\Pi}_{\Delta\Lambda} \approx [\mathbf{1}\cosh(\Delta\Lambda)+\boldsymbol{\sigma}_1\sinh(\Delta\Lambda)] \quad (37)$$

and

$$\mathbf{\Pi}_{\Delta\Phi} \approx [\mathbf{1}\cos(\Delta\Phi)+\mathrm{i}\boldsymbol{\sigma}_2\sin(\Delta\Phi)] \quad , \quad (38)$$

respectively. The propagator matrix along the ray can be composed of propagator matrices corresponding to the individual "high–velocity" segments $\mathbf{\Pi}_{\Delta\Lambda}$ and "low–velocity" segments $\mathbf{\Pi}_{\Delta\Phi}$,

$$\mathbf{\Pi} = \mathbf{\Pi}_{\Delta\Phi_N}\mathbf{\Pi}_{\Delta\Lambda_N}...\mathbf{\Pi}_{\Delta\Phi_2}\mathbf{\Pi}_{\Delta\Lambda_2}\mathbf{\Pi}_{\Delta\Phi_1}\mathbf{\Pi}_{\Delta\Lambda_1}\mathbf{\Pi}_{\Delta\Phi_0} \quad , \quad (39)$$

i.e.,

$$\begin{aligned} \mathbf{\Pi} \approx\ & [\mathbf{1}\cos(\Delta\Phi_N)+\mathrm{i}\boldsymbol{\sigma}_2\sin(\Delta\Phi_N)]\,[\mathbf{1}\cosh(\Delta\Lambda_N)+\boldsymbol{\sigma}_1\sinh(\Delta\Lambda_N)] \\ & \times ... \\ & \times [\mathbf{1}\cos(\Delta\Phi_2)+\mathrm{i}\boldsymbol{\sigma}_2\sin(\Delta\Phi_2)]\,[\mathbf{1}\cosh(\Delta\Lambda_2)+\boldsymbol{\sigma}_1\sinh(\Delta\Lambda_2)] \\ & \times [\mathbf{1}\cos(\Delta\Phi_1)+\mathrm{i}\boldsymbol{\sigma}_2\sin(\Delta\Phi_1)]\,[\mathbf{1}\cosh(\Delta\Lambda_1)+\boldsymbol{\sigma}_1\sinh(\Delta\Lambda_1)] \\ & \times [\mathbf{1}\cos(\Delta\Phi_0)+\mathrm{i}\boldsymbol{\sigma}_2\sin(\Delta\Phi_0)] \quad . \end{aligned} \quad (40)$$

Taking only the terms with cosines for $\Delta\Phi_n$, $n = 1, 2, ..., N-1$, we arrive at the zero–order approximation of the right–hand side of (40),

$$\mathbf{\Pi}^{(0)} = \prod_{n=1}^{N-1} \cos(\Delta\Phi_n) \left[\mathbf{1} \cosh\left(\sum_{n=1}^{N} \Delta\Lambda_n \right) \cos(\Delta\Phi_N + \Delta\Phi_0) \right.$$
$$\left. + \boldsymbol{\sigma}_3 \sinh\left(\sum_{n=1}^{N} \Delta\Lambda_n \right) \sin(\Delta\Phi_N - \Delta\Phi_0) \right] + \boldsymbol{\sigma}_1 ... + \boldsymbol{\sigma}_2 ... \,. \quad (41)$$

The correction with one cosine term replaced by the sine term for $\Delta\Phi_J$ is

$$\mathbf{\Pi}^{(J)} = \frac{\sin(\Delta\Phi_J)}{\cos(\Delta\Phi_J)} \prod_{n=1}^{N-1} \cos(\Delta\Phi_n)$$
$$\times \left[-\mathbf{1} \cosh\left(\sum_{n=J}^{N} \Delta\Lambda_n - \sum_{n=1}^{J-1} \Delta\Lambda_n \right) \sin(\Delta\Phi_N + \Delta\Phi_0) \right.$$
$$\left. + \boldsymbol{\sigma}_3 \sinh\left(\sum_{n=J}^{N} \Delta\Lambda_n - \sum_{n=1}^{J-1} \Delta\Lambda_n \right) \cos(\Delta\Phi_N - \Delta\Phi_0) \right] + \boldsymbol{\sigma}_1 ... + \boldsymbol{\sigma}_2 ... \,. \quad (42)$$

The correction with two cosine terms replaced by the sine terms for $\Delta\Phi_J$ and $\Delta\Phi_K$ is

$$\mathbf{\Pi}^{(JK)} = \frac{\sin(\Delta\Phi_J)\sin(\Delta\Phi_K)}{\cos(\Delta\Phi_J)\cos(\Delta\Phi_K)} \prod_{n=1}^{N-1} \cos(\Delta\Phi_n)$$
$$\times \left[-\mathbf{1} \cosh\left(\sum_{n=K}^{N} \Delta\Lambda_n - \sum_{n=J}^{K-1} \Delta\Lambda_n + \sum_{n=1}^{J-1} \Delta\Lambda_n \right) \cos(\Delta\Phi_N + \Delta\Phi_0) \right.$$
$$\left. - \boldsymbol{\sigma}_3 \sinh\left(\sum_{n=K}^{N} \Delta\Lambda_n - \sum_{n=J}^{K-1} \Delta\Lambda_n + \sum_{n=1}^{J-1} \Delta\Lambda_n \right) \sin(\Delta\Phi_N - \Delta\Phi_0) \right]$$
$$+ \boldsymbol{\sigma}_1 ... + \boldsymbol{\sigma}_2 ... \,. \quad (43)$$

Further corrections $\mathbf{\Pi}^{(JKL)}$, $\mathbf{\Pi}^{(JKLM)}$, etc. may be calculated in a similar way.

Since corrections (42) are smaller than zero–order approximation (41) roughly by the factors of $\exp\left[-2\min\left(\sum_{n=J}^{N}\Delta\Lambda_n, \sum_{n=1}^{J-1}\Delta\Lambda_n\right)\right]$ and corrections (43) are smaller roughly by the factors of $\exp\left(-2\sum_{n=J}^{K-1}\Delta\Lambda_n\right)$, we approximate the propagator matrix by the zero–order approximation only,

$$\mathbf{\Pi}(\tau, \tau_0) \approx \mathbf{\Pi}^{(0)}(\tau, \tau_0) \quad . \quad (44)$$

5.3 Approximation of the Lyapunov exponent

Inserting coefficients Π_0 and Π_3 from (41) into (22) and (25), we approximately obtain

$$L \approx \sum_{n=1}^{N} \Delta\Lambda_n + \sum_{n=1}^{N-1} \ln|\cos(\Delta\Phi_n)| + \tfrac{1}{2}\ln\left[\cos^2(\Delta\Phi_0+\Delta\Phi_N)+\sin^2(\Delta\Phi_0-\Delta\Phi_N)\right] \quad . \tag{45}$$

The mean value of $\ln|\cos(\Delta\Phi_n)|$ over all values of angle $\Delta\Phi_n$ is

$$\langle \ln|\cos(\Delta\Phi_n)|\rangle = -\ln 2 \tag{46}$$

and the standard deviation of $\ln|\cos(\Delta\Phi_n)|$ from the mean value is

$$\sqrt{\left\langle \left[\ln|\cos(\Delta\Phi_n)| - \langle \ln|\cos(\Delta\Phi_n)|\rangle\right]^2 \right\rangle} = \frac{\pi}{\sqrt{12}} \quad . \tag{47}$$

Because of rough approximation (38) of the argument $\Delta\Phi_n$ of the cosine, the cosine is considerably inaccurate for Φ_n comparable with $\frac{\pi}{2}$ and greater. We thus replace the $\ln|\cos(\Delta\Phi_n)|$ for $\Delta\Phi_n > \frac{\pi}{3}$ with its mean value,

$$\Delta\Phi_n \longrightarrow \min\left(\Delta\Phi_n, \frac{\pi}{3}\right) \quad , \qquad n = 1, 2, ..., N-1 \quad . \tag{48}$$

Similarly, the mean value of the last addend in (45) over all angles $\Delta\Phi_0$ and $\Delta\Phi_N$ is

$$\begin{aligned}
&\left\langle \tfrac{1}{2}\ln\left[\cos^2(\Delta\Phi_0+\Delta\Phi_N)+\sin^2(\Delta\Phi_0-\Delta\Phi_N)\right]\right\rangle \\
&\quad = \left\langle \tfrac{1}{2}\ln\left[1-\sin(2\Delta\Phi_0)\sin(2\Delta\Phi_N)\right]\right\rangle = \left\langle \tfrac{1}{4}\ln\left[1-\sin^2(2\Delta\Phi_0)\sin^2(2\Delta\Phi_N)\right]\right\rangle \\
&\quad = \left\langle \tfrac{1}{2}\ln\left\{\tfrac{1}{2}\left[1+\cos^2(2\Delta\Phi_N)\right]\right\}\right\rangle = \langle \ln|\cos(\Delta\Phi_N)|\rangle = -\ln 2 \ .
\end{aligned} \tag{49}$$

The mean value is reached if both $\Delta\Phi_0 = \frac{\pi}{6}$ and $\Delta\Phi_N = \frac{\pi}{6}$. We thus replace

$$\Delta\Phi_n \longrightarrow \min\left(\Delta\Phi_n, \frac{\pi}{6}\right) \quad , \qquad n = 0, N \quad . \tag{50}$$

Finally,

$$\boxed{\begin{aligned}
L \approx &\sum_{n=1}^{N} \Delta\Lambda_n + \sum_{n=1}^{N-1} \ln\left|\cos\left[\min\left(\Delta\Phi_n, \frac{\pi}{3}\right)\right]\right| \\
&+ \frac{1}{2}\ln\left\{1-\sin\left[2\min\left(\Delta\Phi_0,\frac{\pi}{6}\right)\right]\sin\left[2\min\left(\Delta\Phi_N,\frac{\pi}{6}\right)\right]\right\} \quad . \qquad (51)
\end{aligned}}$$

6 Isotropic medium

In an isotropic medium with Hamiltonian $H = v^2\mathbf{p}^{\mathrm{T}}\mathbf{p}$, the second phase–space derivatives of the Hamiltonian in ray–centred coordinates q_1, q_2 are

$$\mathbf{V} = v^{-1}\begin{pmatrix} \frac{\partial^2 v}{\partial q^1 \partial q^1} & \frac{\partial^2 v}{\partial q^1 \partial q^2} \\ \frac{\partial^2 v}{\partial q^1 \partial q^2} & \frac{\partial^2 v}{\partial q^2 \partial q^2} \end{pmatrix} \tag{52}$$

and

$$\mathbf{G} = v^2\mathbf{1} \quad . \tag{53}$$

In 2-D, parameters (32) and (33) read

$$\Lambda = \int \sqrt{\mathrm{neg}\left(v\frac{\partial^2 v}{\partial q \partial q}\right)}\,\mathrm{d}\tau \tag{54}$$

and

$$\Phi = \int \sqrt{\mathrm{pos}\left(v\frac{\partial^2 v}{\partial q \partial q}\right)}\,\mathrm{d}\tau \quad , \tag{55}$$

where $\frac{\partial^2 v}{\partial q \partial q}$ is the second derivative of the velocity with respect to in–plane ray–centred coordinate q perpendicular to the ray.

7 Average "Lyapunov exponent" for the model

Our estimation of the "Lyapunov exponent" is dependent on the position and direction of a particular ray. Let us now average the "Lyapunov exponent" over the whole model volume.

We cover the model by a dense system of parallel straight lines. For each direction of the lines, we calculate average "Lyapunov exponent" (26) using equation (51), similarly like for a system of rays. Then we average the calculated "Lyapunov exponent" over the directions, applying a selected directional weighting function. For instance, the weighting function may have the shape of the model box with the origin at the centre of the box or at the mean position of intended point sources. The weighting function may also correspond to the probability of the ray directions estimated for ray tracing in the model. Refer to Figure 4 for the examples of directional dependence of the average "Lyapunov exponent" and for the directional weighting function.

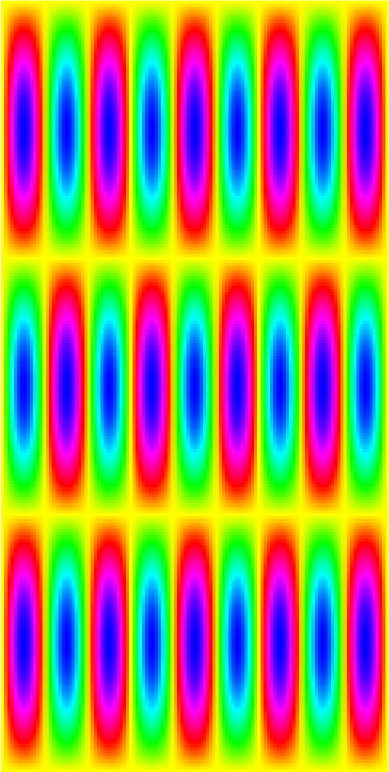

Figure 1. The model is formed by the homogeneous background of velocity $1.0\,\mathrm{km\,s^{-1}}$, perturbed by stretched bi–sine egg–box of amplitude $0.2\,\mathrm{km\,s^{-1}}$. The horizontal dimension of the model box is 3 km, vertical 6 km. The zones situated close to the four corners are low–velocity zones.

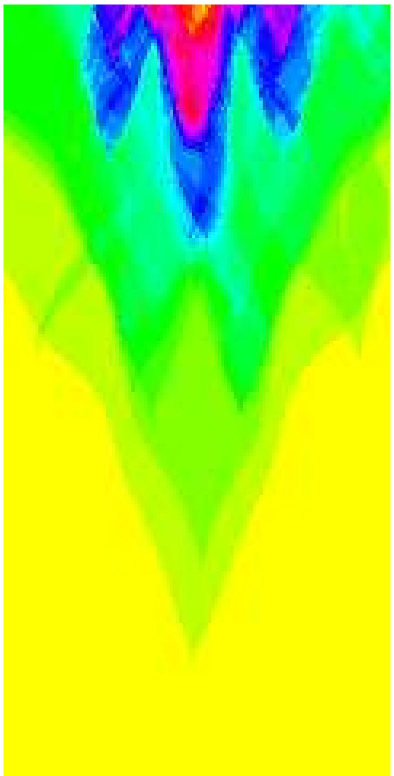

Figure 2. The numbers of travel times corresponding to the point source situated at the bottom of the model box, 1.55 km from the left–hand corner. The maximum number of found travel times is 49.

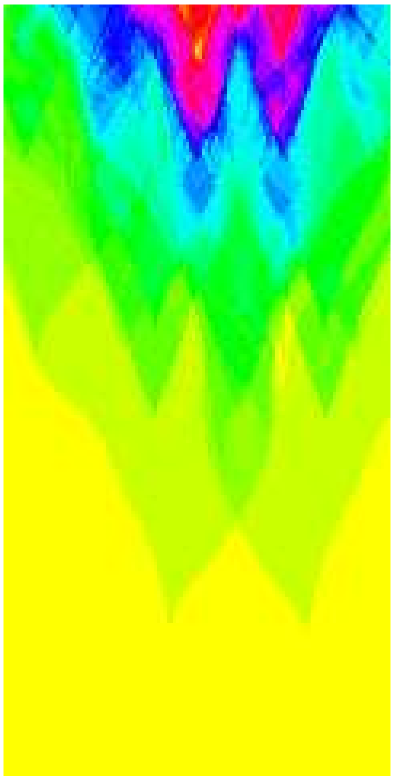

Figure 3. The numbers of travel times corresponding to the point source situated at the bottom of the model box, 1.85 km from the left–hand corner. The maximum number of found travel times is 59.

8 Numerical example

The model designed by Jean–David Benamou is formed by the homogeneous background of velocity $1.0\,\mathrm{km\,s^{-1}}$, perturbed by stretched bi–sine egg–box of amplitude $0.2\,\mathrm{km\,s^{-1}}$, see Figure 1. The horizontal dimension of the model box is 3 km, vertical 6 km. There are low–velocity zones close to the four corners. Average travel times in seconds closely correspond to average lengths in kilometres in this model.

Figure 2 displays the numbers of travel times corresponding to the point source situated at the bottom of the model box, 1.55 km from the left–hand corner. The travel times are calculated on the grid of 121×241 points covering the model box. The maximum number of found travel times is 49. Figure 3 shows the numbers of travel times for the point source shifted to 1.85 km from the left–hand corner. The maximum number of found travel times is 59.

Ninety directions with the angular increment of 2 degrees have been chosen for the estimation of the average "Lyapunov exponent" for the model. For each direction, the model has been covered by 45 equally spaced straight lines. The "Lyapunov exponent" according to equations (23) and (51) has been numerically calculated with the step corresponding to 45 steps along the longest line for the direction. The average "Lyapunov

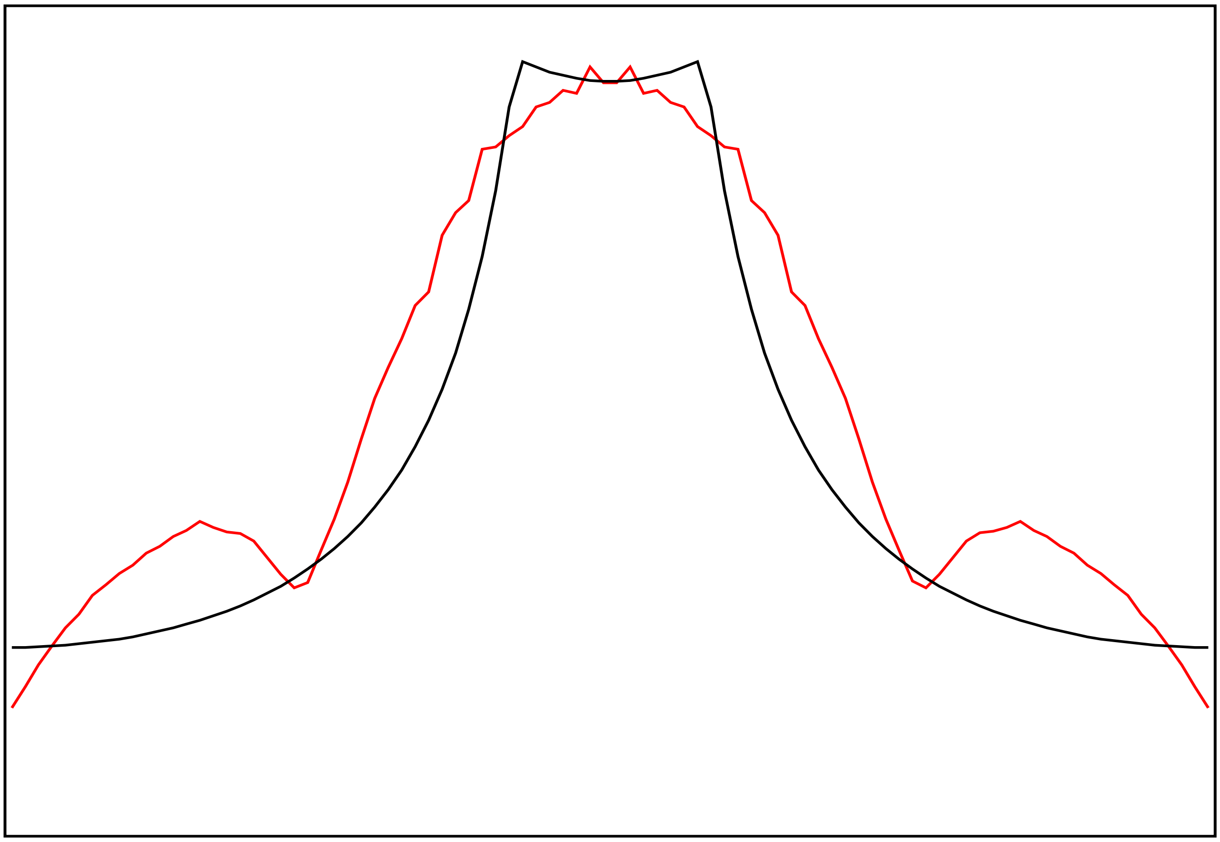

Figure 4. The angular dependence of the average "Lyapunov exponents" for the model [*red*] and the selected directional weighting function [*black*]. The extent of the horizontal axis is 180 degrees, with the vertical direction at its centre. The average "Lyapunov exponents" vary between $0.170\,\mathrm{s}^{-1}$ and $1.019\,\mathrm{s}^{-1}$. The selected directional weighting function corresponds to the model box with the origin at the centre of the bottom edge, see Figure 1. Let us emphasize that the red line describes the velocity heterogeneities whereas the black line characterizes the shape of the model box.

exponent" for each direction has been calculated according to equation (26), with respect to travel time, $\sigma(\tau) = \tau$. Since the statistical properties of the model are strongly anisotropic, the average "Lyapunov exponents" vary between $0.170\,\mathrm{s}^{-1}$ and $1.019\,\mathrm{s}^{-1}$ for different directions, see the red function in Figure 4. The selected directional weighting function corresponds to the model box with the origin at the centre of the bottom edge, see the black function in Figure 4. Such a directional weighting function is suitable for the point sources situated at the bottom or at the top of the model box. The average "Lyapunov exponent" for the model, calculated with this directional weighting function, is

$$\overline{\lambda}_{\mathrm{model}} = 0.698\,\mathrm{s}^{-1} \quad . \tag{56}$$

The average "Lyapunov exponent" does not noticeably vary with the horizontal translation of the origin of the directional weighting function within the middle third of the horizontal model dimension.

Figure 5 shows the behaviour of logarithm (25) of the "norm" (22) of the paraxial–ray propagator matrix along individual rays shot from the second source (1.85 km). Note that the values of logarithms at the endpoints of the rays have been inserted into equation (26) to calculate the average "Lyapunov exponent" corresponding to the source.

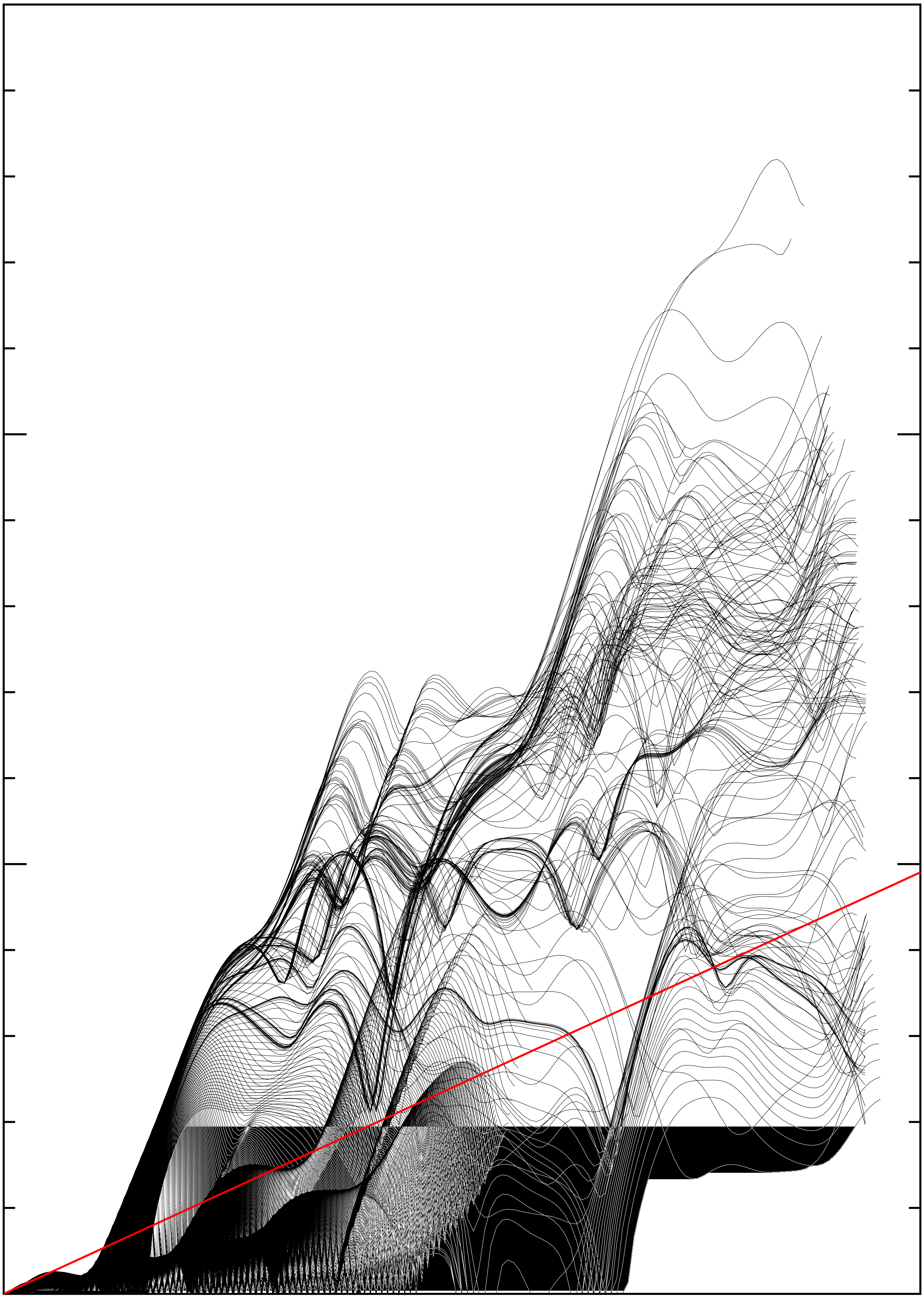

Figure 5. The behaviour of logarithm (25) of the "norm" (22) of the paraxial–ray propagator matrix along individual rays shot from the source of Figure 3. The horizontal axis represents travel time and extends from 0 s to 8 s. The vertical axis represents the natural logarithm and extends from 0 to 15. The red line corresponds to average "Lyapunov exponent" $0.613\,\mathrm{s}^{-1}$ for this set of rays.

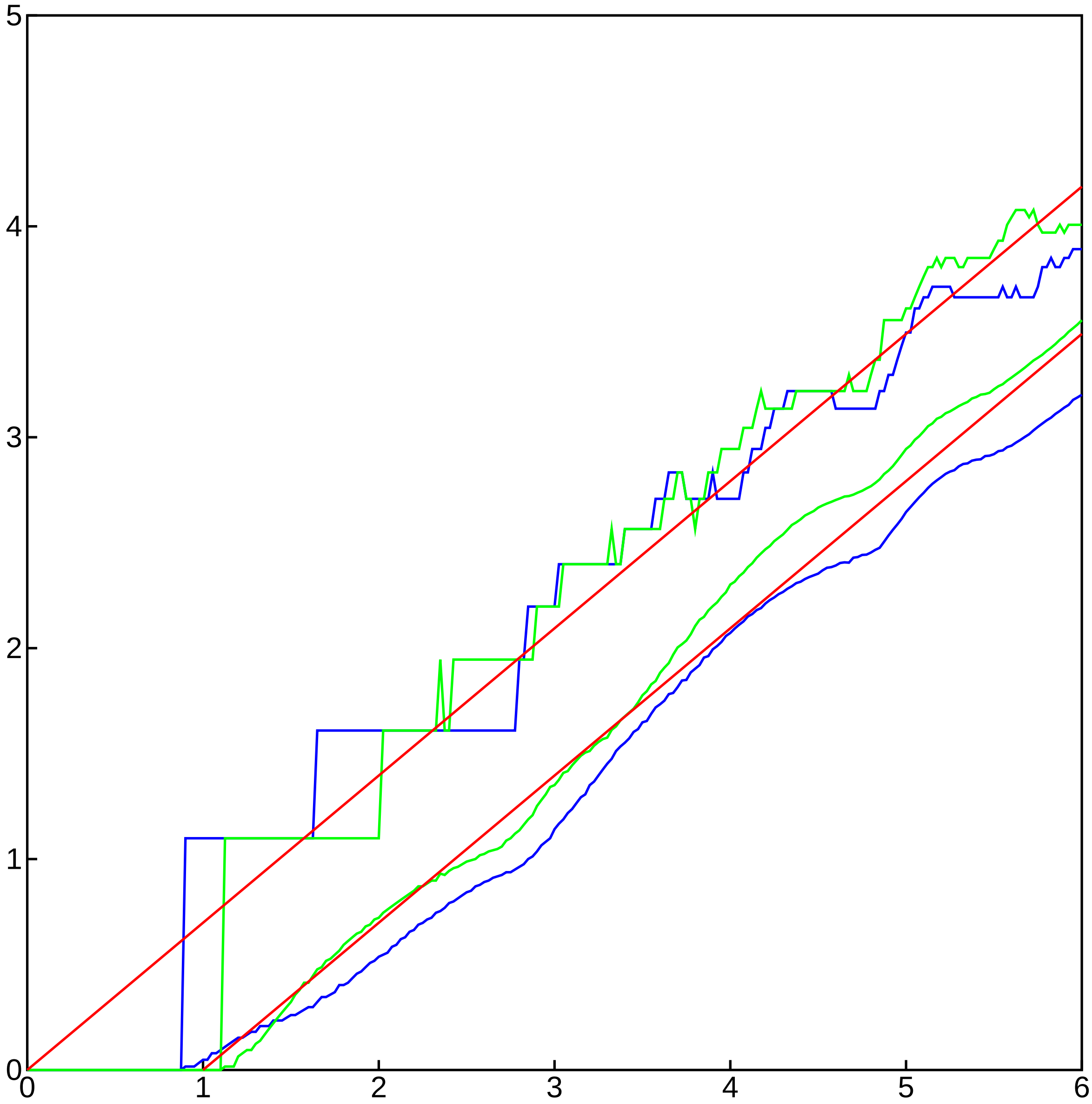

Figure 6. The natural logarithms of the average and maximum numbers of travel times along individual horizontal gridlines of Figure 2 [*blue*] and Figure 3 [*green*]. The horizontal axis represents the distance of a gridline from the bottom of the model box in kilometres, and serves as a rough approximation to the travel time in seconds. The slope of the red line is given by average "Lyapunov exponent" (56) for the model.

The average "Lyapunov exponent", calculated for the rays traced from the first source (1.55 km) according to equations (22), (25) and (26), using the paraxial–ray propagator matrix, is $0.679\,\mathrm{s}^{-1}$. The average "Lyapunov exponent" estimated along the same rays using equation (51) is $0.676\,\mathrm{s}^{-1}$. However, the standard deviation between equation (25) and approximation (51) for individual rays is considerably greater than the estimation based on equation (47). This could be explained if the standard deviations of approximations (37), (38) or (44) were comparable with the standard deviation (47) of approximations (48) and (50).

The average "Lyapunov exponent" calculated for the rays traced from the second source (1.85 km) according to equations (22), (25) and (26), using the paraxial–ray propagator matrix, is $0.613\,\mathrm{s}^{-1}$. The average "Lyapunov exponent" estimated along the same rays using equation (51) is $0.697\,\mathrm{s}^{-1}$.

Figure 6 displays, in blue and green, the natural logarithms of the average and maximum numbers of travel times along individual horizontal gridlines of Figures 2 and 3. The horizontal axis is the distance of a gridline from the bottom of the model box in kilometres, and serves as a rough approximation to the travel time in seconds. The slope of the red line is given by average "Lyapunov exponent" (56) for the model.

If the numerical example is correct (last–minute calculations), it demonstrates a good correspondence between the average logarithms of the numbers of ray–theory travel times, the average "Lyapunov exponents" for the rays and the estimation of the average "Lyapunov exponent" for the model.

References

Klimeš, L. (1994): Transformations for dynamic ray tracing in anisotropic media. Wave Motion, **20**, 261–272.

Matyska, C. (1999): Note on chaos in ray propagation. In: Seismic Waves in Complex 3-D Structures, Report 8, pp. 71–82, Dep. Geophys., Charles Univ., Prague.